Establishment of a virulent full-length cDNA clone for type I feline coronavirus strain C3663

Yutaka Terada[a,b], Yudai Kuroda[b], Shigeru Morikawa[c], Yoshiharu Matsuura[d], Ken Maeda[b,c] and Wataru Kamitani[a]#

[a]Laboratory of Clinical Research on Infectious Diseases, Research Institute for Microbial Diseases, Osaka University, Osaka, Japan

[b]Laboratory of Veterinary Microbiology, Joint Faculty of Veterinary Medicine, Yamaguchi University, Yamaguchi, Japan

[c]Department of Veterinary Science, National Institute of Infectious Diseases, Tokyo, Japan.

[d]Department of Molecular Virology, Research Institute for Microbial Diseases, Osaka University, Osaka, Japan

Running Head: Infectious cDNA clone of virulent type I FCoV

#Address correspondence to Wataru Kamitani, DVM, PhD, wakamita@biken.osaka-u.ac.jp.

Abstract word count: 236 words

Text word count: 9531 words

Number of pages: 35

Number of figures: 5

Abstract

Feline infectious peritonitis (FIP) is one of the most important infectious diseases in cats and is caused by feline coronavirus (FCoV). Tissue culture-adapted type I FCoV shows reduced FIP induction in experimental infections, which complicates the understanding of FIP pathogenesis caused by type I FCoV. We previously found that the type I FCoV strain C3663 efficiently induces FIP in specific pathogen free cats through the naturally infectious route. In this study, we employed a bacterial artificial chromosome-based reverse genetics system to gain more insights into FIP caused by the C3633 strain. We successfully generated recombinant virus (rC3663) from Fcwf-4 cells transfected with infectious cDNA that showed similar growth kinetics to the parental virus. Next, we constructed a reporter C3663 virus carrying the nanoluciferase (Nluc) gene to measure viral replication with high sensitivity. The inhibitory effects of different compounds against rC3663-Nluc could be measured within 24 h post-infection. Furthermore, we found that A72 cells derived from canine fibroblasts permit FCoV replication without apparent cytopathic effects. Thus, our reporter virus is useful for uncovering the infectivity of type I FCoV in different cell lines, including canine-derived cells. Surprisingly, we uncovered aberrant viral RNA transcription of rC3663 in A72 cells. Overall, we succeeded in obtaining infectious cDNA clones derived from type I FCoV that retained its virulence. Our recombinant FCoVs are powerful tools for increasing our understanding of the viral life cycle and pathogenesis of FIP-inducing type I FCoV.

Importance

Feline coronavirus (FCoV) is one of the most significant coronaviruses,

because this virus induces feline infectious peritonitis (FIP), which is lethal disease in cats. Tissue culture-adopted type I FCoV often loses pathogenicity, which complicates research on type I FCoV-induced feline infectious peritonitis (FIP). Since we previously found that the type I FCoV strain C3663 efficiently induces FIP in specific pathogen free cats, we established a reverse genetics system for the C3663 strain to obtain recombinant viruses in the present study. By using a reporter C3663 virus, we were able to examine the inhibitory effect of 68 compounds on C3663 replication in Fcwf-4 cells and infectivity in a canine-derived cell line. Interestingly, one canine cell line, A72, permitted FCoV replication but with low efficiency and aberrant viral gene expression.

Introduction

Coronaviruses (CoVs) are pathogens that infect a wide variety of animals, including humans, and cause respiratory and enteric diseases (1). CoVs are enveloped viruses possessing a large single-stranded, positive sense RNA (~32 kb) (2), are classified as order *Nidovirales*, family *Coronaviridae*, and subfamily *Coronavirinae*. CoVs are further classified into four genera, alpha, beta, gamma, and delta (3). *Feline coronavirus* belongs to alpha CoVs, together with *canine coronavirus*, *porcine transmissible gastroenteritis virus*, *porcine epidemic diarrhea virus*, and *human coronavirus* 229E and NL63 (3).

Feline CoV (FCoV) infections are distributed worldwide in domestic cats and wild Felidae, such as lions (4, 5) and cheetahs (6). Based on their pathogenicity, FCoVs can be classified into two biotypes—feline enteric CoV (FECV) and feline infectious peritonitis virus (FIPV). FECV infections are asymptomatic or occasionally induce mild intestinal inflammation in kittens (7). On the other hand, FIPV infections induce the more severe and immune-mediated lethal disease, feline infectious peritonitis (FIP) (8, 9).

FCoVs can also be further classified into two types, types I and II, based on their antigenicity (10, 11). Unlike type II FCoV, type I FCoV infections occur predominantly in felids worldwide (12-14). Furthermore, their virological features differ, including growth characteristics in cell culture and receptor usage (7, 15). Compared with type I FCoV, type II FCoV shows better growth kinetics and can more easily induce FIP in specific pathogen free (SPF) cats. Despite the fact that type II FCoV infections occur with low frequency, many researchers employ type II FCoVs to analyze FIP pathogenesis. Therefore, a type I FCoV strain that can induce FIP is needed to fully

understand FIP pathogenesis.

It has been proposed that type I FECV replicates and acquires mutations in its viral genome in kittens, and then, the mutated FECV becomes a FIP-associated virus. This hypothesis is known as the “internal mutation theory” (16-18), which is supported by the proposal of virulent FIP markers. Based on epidemiological studies, spike (S) and/or open reading frame (ORF) 3c genes of type I FCoV are thought to be virulent markers (18-20). However, none of the proposed markers have been proven virulent owing to the lack of feasible FIP cat models with type I FCoV. It is difficult for most type I FCoVs isolated from FIP cats to induce FIP in experimental settings using SPF cats. It is thought that adaptation of type I FCoV in tissue culture results in the loss of pathogenicity (21, 22).

Recently, we discovered a strain of type I FCoV, C3663, isolated from FIP cats (23) that retained virulence despite adaptation in Fcwf-4 cells (9). Surprisingly, three of four SPF cats (75%) developed FIP after infection with the C3663 strain (9). These findings suggest that our C3663 strain is a candidate for analyzing FIP pathogenesis induced by type I FCoV in experimental settings.

In this study, we constructed an infectious cDNA clone derived from the type I FCoV C3663 strain by utilizing the bacterial artificial chromosome (BAC) system. Recombinant C3663 (rC3663) virus was easily rescued from Fcwf-4 cells transfected with BAC plasmids carrying the C3663 full-length genome. rC3663 showed similar growth kinetics to the parental virus. Furthermore, we generated a recombinant virus bearing the nanoluciferase (Nluc) gene in the ORF 3abc region. This rC3663-Nluc reporter virus was useful in investigating the inhibitory effects of compounds and revealed the infectivity of type I FCoV in canine cells. Interestingly, the expression ratio

of subgenomic (sg) mRNA was different in canine-derived A72 cells infected with rC3663 virus, suggesting that aberrant viral RNA transcription of the rC3663 virus occurred in A72 cells.

Results

Construction of BAC carrying the full-length C3663 genome

The full genome sequence of type I FCoV strain C3663 was assembled into the pBeloBAC11 vector to generate infectious cDNA clones under the control of a cytomegalovirus (CMV) immediate-early promoter (Fig. 1A). To this end, we separated the genomic sequence of C3663 into 11 fragments and sequentially assembled them into the BAC plasmid (Fig. 1A). The vector backbone bears the CMV promoter followed by the hepatitis delta virus (HDV) ribozyme and bovine growth hormone (BGH) termination sequences (Fig. 1A); the C3663 genomic sequence was cloned into the pBeloBAC11 vector between the CMV promoter and the 25 nucleotide (nt) poly (A), HDV ribozyme, and BGH termination sequences (Fig. 1A). The full-length infectious cDNA clone was designated pBAC-FCoV-C3663 and sequence analysis showed that it possessed 25 nucleotide mutations compared with that of the C3663 reference sequence (Table 1). Of the 25 mutations, 11 were synonymous and 14 were non-synonymous mutations (Table 1). Two synonymous mutations at nt 9831 and nt 9834 were introduced as the genetic marker, which disrupts the *Eco*RI site (ΔEcoRI), confirming virus recovery from the cDNA clone (Fig. 1B and Table 1).

Virus recovery by pBAC-FCoV-C3663 transfection

We produced rC3663 virus from Fcwf-4 cells, which are highly susceptible to FCoV infection, by transfecting the cells with pBAC-FCoV-C3663. Small cytopathic effects (CPE) were observed 2 days post transfection (dpt), which became larger by 3 dpt. To determine rC3663 virus recovery, we employed RT-PCR on isolated RNA from rC3663 and the parental strain. We further confirmed the ΔEcoRI genetic maker by

analyzing *Eco*RI digestion and Sanger sequencing (Fig. 1C and D). Next, we analyzed the virological features of the rC3663 virus by comparing the growth kinetics of rC3663 and parental C3663 in Fcwf-4 cells after inoculating them with viruses at a multiplicity of infection (MOI) of 0.01. The results showed that rC3663 growth kinetics were similar to that of the parental C3663 (Fig. 1E). Furthermore, we compared viral RNA replication in parental C3663 or rC3663-infected Fcwf-4 cells by northern blot analysis (Fig. 1F) and found that the amount of genomic (g) RNA and sg mRNAs in rC3663-infected Fcwf-4 cells were similar to that of the parental C3663-infected cells (Fig. 1F). Taken together, we were able to successfully generate infectious cDNA clones derived from type I FCoV strain C3663 using the BAC system. Our results indicate that the recovered rC3663 virus possesses identical virological features as the parental C3663 virus. (Fig. 1E and F).

Establishment of reporter rC3663 bearing the Nluc gene

In virology, recombinant viruses carrying reporter genes (GFP, RFP, or luciferase) provide many advantages for analyzing viral characteristics and screening for therapeutic compounds (24, 25). Thus, we attempted to construct an infectious cDNA clone of type I FCoV strain C3663 carrying an Nluc gene. By following the protocols of Tekes et al. (26), we inserted the Nluc gene into pBAC-FCoV-C3663 in place of the ORF 3abc gene to obtain pBAC-FCoV-C3663-Nluc (Fig. 2A). The Nluc gene replaced a region containing the start codon of ORF 3a to 71 nt upstream of the ORF 3c stop codon to retain the transcription regulatory sequence (TRS) of the M gene (Fig. 2A).

To examine Nluc expression in Fcwf-4 cells infected with rC3663-Nluc virus,

we inoculated Fcwf-4 cells with rC3663-Nluc at an MOI of 0.01. Infection with rC3663 was used as control. After 24, 48, and 72 h post-infection (hpi), we found that Nluc activity in rC3663-Nluc-infected Fcwf-4 cells—but not in rC3663 or mock-infected cells—increased in a time-dependent manner (Fig. 2B).

We further investigated the viral growth of rC3663-Nluc in Fcwf-4 cells by harvesting the supernatants of rC3663-Nluc or rC3663-infected Fcwf-4 cells at 24, 48, and 72 hpi and then determining infectious titers of the supernatants by plaque assays. The production of infectious virus particles from rC3663-Nluc-infected cells was comparable to that of rC3663-infected cells (Fig. 2C). As shown in Fig. 2B and 2C, the increase in Nluc activity was significantly correlated with viral replication in rC3663-Nluc-infected cells. Our data indicate that rC3663 carrying the Nluc reporter gene is a powerful tool for investigating type I FCoV viral replication and production.

Application of the rC3663 reporter virus in compound screening

Before applying the rC3663 reporter virus to compound screening, we determined sensitivity of the rC3663-Nluc virus to treatment with known inhibitors of CoV replication, cyclosporine A (27, 28) and lopinavir (29). After adsorption of rC3663-Nluc onto Fcwf-4 cells at an MOI of 0.01, the infected cells were treated with various concentrations of cyclosporine A or lopinavir. As shown in Fig. 2D and 2E, both compounds inhibited luciferase activity in a dose-dependent manner. Furthermore, viral RNA levels in cyclosporine A or lopinavir-treated cells were measured by real-time RT-PCR (Fig. 2D and 2E). Intracellular viral RNA levels were found reduced in a dose-dependent manner for both compounds and were correlated with luciferase activity, suggesting that detection sensitivity of luciferase expression in

rC3663-Nluc-infected cells is comparable to that of viral RNA expression levels.

Next, to determine the usefulness of the rC3663 reporter virus for screening antiviral compounds, we utilized a commercially available library of 68 protease inhibitors. Fcwf-4 cells were inoculated with rC3663-Nluc (MOI = 0.01) and 10 μM of each protease inhibitor; cyclosporine A and DMSO were used as positive and negative control, respectively. The side effects of protease inhibitors were determined by MTT assays (Fig. 2F). Together with the MTT assay results, 15 inhibitors were found to exhibit more than 75% reduction in Nluc activity compared with that of the DMSO control and without any accompanying cytotoxicity (Fig. 2F; compound no. 2, 25, 29, 31, 34, 35, 48, 50, 56, 58, 64–67, and 69). Indeed, compound no. 31 (lopinavir) inhibited luciferase activity, which is consistent with the results in Fig. 2E. Overall, our results support the suitability of rC3663-Nluc in compound screening.

Identification of permissive cell lines for type I FCoV

In vitro propagation of type I FCoV is limited to a few cell lines, including Fcwf-4 cells, AKD cells, and CRFK cells, because type I FCoV only shows a CPE in such cell lines (23, 30, 31) . Thus, it is difficult to investigate the infectivity of type I FCoV in cell lines derived from other animals, such as dogs. Nevertheless, we explored novel cell lines for propagation of type I FCoV by inoculating three canine-derived cell lines, A72 (canine fibroblasts), MDCK (canine kidney epithelial cells), and DH82 (canine macrophages), with the rC3663-Nluc virus (MOI = 0.1) and investigated infectivity by measuring Nluc activity. Although a CPE was not observed for rC3663-Nluc-infected A72 cells, Nluc activity was significantly high at 24 hpi and increased in a time-dependent manner (Fig. 3A and C). On the other hand,

rC3663-Nluc-infected MDCK and DH82 cells did not exhibit detectable Nluc activity (Fig. 3B).

To determine viral RNA replication in A72 cells, A72, MDCK, DH82, and Fcwf-4 cells were infected with rC3663-Nluc virus at an MOI of 0.01, followed by real-time RT-PCR analysis of RNA extracted at 24, 48, and 72 hpi. Although the amount of viral RNA in rC3663-Nluc-infected A72 cells was lower than in Fcwf-4 cells, the amount of viral RNA in A72 cells (but not in DH82 and MDCK cells) was still significantly high at 48 and 72 hpi (Fig. 3D). These results indicate that A72 cells permit replication of type I FCoV C3663 virus.

Next, we determined the production of infectious virus particles from rC3663-Nluc-infected A72 cells by collecting the culture supernatants at 24, 48, and 72 hpi and measuring viral titers by plaque assays with Fcwf-4 cells (Fig. 3E). The supernatant infectious titers of Fcwf-4 cells reached 1.67×10^5 PFU/mL at 72 hpi and the amount of viral RNA determined by real-time RT-PCR increased in a time-dependent manner in Fcwf-4 cells (Fig. 3D and E). As shown in Fig. 3A and D, A72 cells support rC3663 virus replication, but the production of infectious viruses was lower compared with that of Fcwf-4 cells. Meanwhile, infectious viruses were not produced by infected MDCK and DH82 cells (Fig. 3E). These results indicate that A72 cells produce progeny viruses—albeit with low efficiency—while MDCK and DH82 cells are not permissive cell lines for type I FCoV.

To further determine the low production of progeny virus by rC3663-Nluc-infected A72 cells, we examined the propagation of rC3663 virus (MOI = 0.1) in A72 and Fcwf-4 cells by indirect immunofluorescence assays (IFA) using confocal microscopy analysis. Using an anti-FCoV N monoclonal antibody, N protein

expression in A72 cells was observed by IFA and exhibited small foci 48 hpi, compared with that of Fcwf-4 cells (Fig. 3F). Therefore, infectious particles were found generated in A72 cells with a low efficiency of infection expansion by progeny particles to neighboring cells. We also examined N protein expression levels using immunoblotting. As expected, N protein expression levels in rC3663 virus-infected A72 cells were significantly low (Fig. 3G). Although the production of progeny virus and N protein was low, our results suggest that canine-derived A72 cells are a permissive cell line for type I FCoV infections without cytotoxic effects.

MDCK cells do not permit viral replication during type I FCoV infection

As shown in Fig. 3 and unlike A72 cells, neither viral RNA replication nor progeny virus production was observed in MDCK and DH82 cells infected with rC3663 virus. These results led us to speculate that the entry receptor for type I FCoV is perhaps not expressed in MDCK and DH82 cells or that viral RNA replication of type I FCoV is not permitted in these cell lines. Unfortunately, the type I FCoV receptor remains unknown. Thus, we examined viral replication levels in cells transfected with pBAC-FCoV-C3663-Nluc. As a negative control, we generated pBAC-FCoV-C3663-Nluc-PolDead by mutating the active site of viral RNA-dependent RNA polymerase (RdRp: nsp12) from SDD to SAA (Fig. 4A) and confirmed that virus rescue did not occur in Fcwf-4 cells transfected with pBAC-FCoV-C3663-Nluc-PolDead because of disrupted RdRp activity (data not shown). After transfecting MDCK cells with pBAC-FCoV-C3663-Nluc or pBAC-FCoV-C3663-Nluc-PolDead together with pcDNA3.1-fluc, we determined luciferase activity in cell lysates at 24, 48 and 72 h p-transfection (Fig. 4B); the firefly

luciferase reporter plasmid pcDNA3.1-fluc (32) was used as an internal control. As shown in Fig. 4B, Nluc expression levels in cells transfected with pBAC-FCoV-C3663-Nluc were comparable to those of pBAC-FCoV-C3663-Nluc-PolDead. Consistent with the luciferase assay results (Fig. 4B), no progeny virus was produced in MDCK cells transfected with pBAC-FCoV-C3663-Nluc (Fig. 4C). In addition, an increase in viral RNA levels (Fig. 4D) as well as N protein expression (Fig. 4E) were not observed in MDCK cells transfected with pBAC-FCoV-C3663-Nluc. Thus, our results indicate that MDCK cells do not permit replication of C3663 virus RNA.

Aberrant expression of type I FCoV viral RNA in A72 cells

As shown in Fig. 3G, expression levels of N protein in infected A72 cells were significantly low. Thus, to determine expression levels of sg N mRNA (sg mRNA6), total RNA extracted from rC3663 virus or mock-infected Fcwf-4 and A72 cells at 48 and 72 hpi were subjected to northern blot analysis with a specific type I FCoV 3′-untranslated region (UTR) probe (Fig. 5A). We found that all viral RNAs, including gRNA and sg mRNA2–7, were detected in Fcwf-4 cells infected with rC3663 virus (Fig. 5A). However, expression levels of gRNA and sg mRNA2–5 were significantly lower in infected A72 cells than those in infected Fcwf-4 cells (Fig. 5A).

Next, to determine the specific RNA signal in infected A72 cells, we generated a set of specific DIG-labeled RNA probes against S, 3abc, M, and N genes (Fig. 5B). As shown in Fig. 5C, we identified seven-specific viral mRNA (gRNA and sg mRNA2–7) using a combination of S, 3abc, M, and N-specific RNA probes in infected Fcwf-4 cells. An unexpected RNA signal was observed between sg mRNA6 and sg mRNA7 (Fig. 5C).

These results indicate that the two RNAs detected in A72 cells infected with rC3663 are sg mRNA6 and sg mRNA7.

We further examined the expression levels of viral sg mRNAs in cells infected with the parental C3663 strain or type I FCoV strain Yayoi using northern blot analysis with specific RNA probes against the 3′-UTR. Although gRNA and sg mRNA2–7 were detected in Fcwf-4 cells infected with C3663 or Yayoi, two specific mRNAs—sg mRNA6 and sg mRNA7—were observed in A72 cells infected with C3663 or Yayoi (Fig. 5A). These results suggest that the decreased synthesis of viral mRNAs is not specific to the infectious clone of C3663.

Although expression levels of sg mRNA6 and sg mRNA7 in A72 cells infected with rC3663 was low (Fig. 5A), the expression ratio between sg mRNA6 and sg mRNA7 in infected A72 cells was different from that of infected Fcwf-4 cells. The relative level of sg mRNA7 in infected A72 cells based on the level of sg mRNA6 was lower than that in infected Fcwf-4 cells (Fig. 5A). To compare these ratios, we used a lower amount of total RNA extracted from infected Fcwf-4 cells for northern blot analysis to adjust the expression levels of sg mRNA6 between infected Fcwf-4 and A72 cells. As a result, sg mRNA6 expression levels in A72 cells were identical to those in Fcwf-4 cells, whereas sg mRNA7 expression levels in A72 cells were lower than in Fcwf-4 cells (Fig. 5D). These findings indicate that aberrant expression of viral RNA occurred in infected A72 cells.

Discussion

Epidemiological research conducted on type I FCoV has proposed virulent factor(s) in its viral genome (19, 20). However, the experimental confirmation of

virulent factor(s) is difficult *in vivo* due to the lack of a feasible FIP cat model of type I FCoV. Recently, we found that the type I FCoV strain C3663 has the ability to induce FIP in SPF cats (9). Thus, in the present study, we constructed an infectious cDNA clone derived from the virulence-retaining type I FCoV strain C3663 by utilizing the BAC system. As a result, we successfully rescued recombinant type I FCoV by transfection of the BAC cDNA clone into Fcwf-4 cells, where the recovered rC3663 showed similar growth kinetics to the parental virus (Fig. 1). In addition, we generated recombinant type I FCoV carrying Nluc as a reporter gene and applied our reporter rC3663 virus to drug screening (Fig. 2).

Several host proteases, such as furin, TMPRSS2, and cathepsins, are required for the entry step of CoVs by cleaving spike proteins at the cell surface or in endosomes (33). Yamamoto et al. (34) showed that nafamostat inhibited MERS-CoV infection by inhibiting TMPRSS2. Consistent with these findings, we identified nafamostat mesylate (compound no. 38) as an FCoV inhibitor without any cytotoxic effects, suggesting that FCoV utilizes the host protease TMPRSS2 for entry. Another compound, lopinavir, is an inhibitor of the human immunodeficiency virus (HIV)-1 protease and is used for acquired immune deficiency syndrome (AIDS) treatment (35). In coronavirus infections, lopinavir inhibits Middle East respiratory syndrome (MERS)-CoV, severe acute respiratory syndrome (SARS)-CoV, and human CoV (HCoV) 229E infection by inhibiting the CoV 3C-like protease (29). HCoV-229E belongs to the same genus as FCoV—*Alphacoronavirus* (3). Unsurprisingly, we identified lopinavir (compound no. 31) as an FCoV inhibitor that does not exhibit cytotoxicity. Our results suggest nafamostat and lopinavir as potential therapeutic agents against FCoV infection.

Specific chemical compounds that are active against type I FCoV can be applied in two different strategies against FIP, cure and prevention. Several studies have attempted to develop curative therapeutic agents against FIP (36-38), and although these compounds suppressed FCoV replication *in vitro*, the compounds failed to suppress FIP *in vivo* (39, 40). While differences between the *in vitro* and *in vivo* activities of these compounds remains controversial, the highly complicated pathological mechanism of FIP, such as antibody dependent enhancement of infection (ADE) (41, 42) and type III hypersensitivity (43, 44), makes developing efficient and curative therapeutics against FIP difficult.

On the other hand, the emergence mechanism of FIPV is best explained by an internal mutation theory (16-18) where type I FCoV has the potential to become type I FIPV by acquiring mutations in its viral genome during replication in kittens. Therefore, controlling the viral load of type I FCoV in kittens is important in preventing FIP disease-onset. If chemical compounds can suppress the viral load of type I FCoV in kittens, then the probability of disease-onset should be reduced. Thus, therapeutics against type I FCoV would be an efficient method of controlling FIP. In this regard, our reporter virus is a powerful tool for finding compounds for use in the cure and/or prevention of FIP as the virus can be utilized in high-throughput screening.

Several reports have addressed the possibility that some viruses among alphacoronavirus-1, such as type II FCoV (45, 46), type I canine CoV (CCoV) (47), and type IIb CCoV (48), emerged as chimeric viruses via recombination events. Feline aminopeptidase N (APN) works as a viral receptor for type II CCoV and porcine transmissible gastroenteritis virus (TGEV) (15, 49) , suggesting that cats and especially kittens play an important role in producing new chimeric viruses. However, the

possibility of recombination in other animals, such as dogs, has not been well-studied. Furthermore, to the best of our knowledge, no reports have shown type I FCoV induction of apparent CPE in cell culture except for Fcwf-4 cells. Indeed, the C3663 strain of type I FCoV did not exhibit CPE in canine-derived cells (Fig. 3C). However, luciferase activity in A72 cells infected with the rC3663-Nluc virus was significantly increased without concomitant CPE (Fig. 3A and 3C), and although progeny virus production was low, A72 cells permitted type I FCoV replication (Fig. 3D). We reasoned that investigating type I FCoV infectivity in other cell lines should not solely rely on CPE-based assays. Furthermore, our findings indicate that recombination events between type I FCoV and CCoV may occur in dogs. Namely, type I FCoV may be transmitted from cats to dogs and a new CoV may emerge in dogs through recombination events. In fact, CCoV replicates in A72 cells (50).

Like other positive-strand viruses, CoVs require host factors for replication (51-53) in infected cells. Unlike A72 cells, MDCK and DH82 cells did not permit viral replication of type I FCoV from pBAC-FCoV-C3663-Nluc (Fig. 3). Thus, we hypothesized that essential host factors exist in canine-derived A72 cells but not in MDCK cells. Future research should elucidate the host factors that support replication of type I FCoV in A72 cells, as these factors would be attractive targets for the development of therapeutics against type I FCoV.

Recently, many researchers have focused on bats as a major reservoir of novel viruses (54). Several novel viruses have been identified and/or isolated from bats and some are related to human pathogenic viruses, such as SARS-CoV (55) and MERS-CoV (56). However, other animal species are also potential novel virus reservoirs; for example, Lau et al. (57) reported that the *Deltacoronavirus* porcine CoV

HKU15 (PorCoV HKU15) can be transmitted from birds to pigs. In addition, HCoV OC43 is known to originate from bovine CoV (58). Therefore, not only bats but other animal species should be investigated for their potential as reservoirs or sources of emerging viruses. Indeed, we found that the canine-derived A72 cell line permits the replication of type I FCoV (Fig. 3). Although host receptors of type I FCoV remain unclear, our reporter virus for FCoV infection may provide insights on viral host jump and emergence of novel viruses.

Generally, expression levels of sg mRNA6 are the highest among all viral mRNA in CoV-infected cells (59) . While sg mRNA6 expression levels in A72 cells were lower than in Fcwf-4 cells, the expression ratio of sg mRNA6 to sg mRNA7 in infected A72 cells was different from that in infected Fcwf-4 cells (Fig. 5A). In fact, expression levels of sg mRNA6 in 2 μg of total RNA extracted from infected A72 cells was similar to its expression levels in 0.05 μg of total RNA extracted from Fcwf-4 cells (Fig. 5D). In contrast, expression levels of sg mRNA7 in A72 cells was lower than in Fcwf-4 cells (Fig. 5D,), suggesting that synthesis of sg mRNAs is impaired in A72 cells.

Our real-time RT-PCR method amplifies the 3′-UTR of viral RNA, which is present in all viral RNAs. Therefore, the increase in viral RNA in A72 cells (Fig. 3D) was possibly caused by the synthesis of sg mRNA6 (Fig. 5A). To our knowledge, there are no reports on aberrant RNA transcription of CoVs in infected cells, such as in A72 cells. Several host proteins, such as the heterogeneous nuclear ribonucleoprotein (hnRNP) family or the DEAD box RNA helicase family, interact with the TRS of CoV RNA and regulate transcription/replication (60). Thus, our data indicate that host factor(s) in Fcwf-4 cells, but not A72 cells, regulate viral RNA transcription. Based on

397 the aberrant expression of viral mRNA in rC3663 virus-infected A72 cells, further
398 studies are required for uncovering the CoV RNA transcription mechanisms in A72
399 cells.

400 In conclusion, we generated recombinant type I FCoV strain C3663 using a
401 BAC-based reverse genetics system. Our recombinant virus can potentially be used to
402 expand research on type I FCoV-induced FIP. Furthermore, the infection of A72 cells
403 with the rC3663 virus revealed unusual viral mRNA expression patterns that may
404 provide novel insights into the mechanisms of CoV transcription. Although further
405 study is required to test whether the recombinant virus can induce FIP *in vivo*, our
406 established type I FCoV clone has the potential to be a powerful tool for understanding
407 FIP pathogenesis. For example, because the S gene is a candidate of FCoV pathogenesis
408 (19, 20), a chimeric S gene virus based on our recombinant virus may provide novel
409 insights into type I FCoV pathogenesis. Additionally, other groups have established type
410 I FCoV reverse genetics using the Black strain (26) and type I field virus (61); thus,
411 exploiting multiple approaches can synergistically further our understanding of FIP.
412
413
414 **Materials and Methods**
415 **Cells and viruses**
416 Cat-derived Fcwf-4 cells (CRL-2787) (9, 62) and the canine-derived cell lines A72
417 (CRL-1542) (63, 64), MDCK (CCL-34) (65), and DH82 (CRL-10389) (66) were grown
418 in Dulbecco's modified Eagle's medium (DMEM; Nacalai Tesque, Kyoto, Japan)
419 supplemented with 10% (for Fcwf-4, A72, and MDCK cells) or 15% (DH82 cells)
420 heat-inactivated fetal bovine serum (FBS), 100 U/mL penicillin, and 100 µg/mL

streptomycin (Nacalai Tesque). Cells were maintained in a humidified 5% CO_2 incubator at 37 °C. The type I FCoV strains C3663 and Yayoi were used in this study (9, 23) and propagated in Fcwf-4 cells as described previously (14).

BAC construction

The BAC DNA of SARS-CoV-Rep (67) was kindly provided by Dr. Luis Enjuanes (Spanish National Center for Biotechnology [CNB-CSIC], Madrid, Spain) and was used as a backbone BAC sequence to generate infectious cDNA carrying the full-length type I FCoV strain C3663 sequence. The full-length genomic sequence of C3663 was divided into eleven fragments that were then assembled into pBeloBAC11 plasmids in a sequential order (Fig. 1A). Fragments Fr1 to Fr11 correspond to nt 11218–13811, nt 13812–16360, nt 16361–18675, nt 18676–20998, nt 20999–23400, nt 23401–26227, nt 9210–11217, nt 26228–28545, nt 1–2069, nt 2070–5152, and nt 5153–9834, respectively. Red/ET recombination was employed for fragment integration with the Red/ET Recombination System Counter-Selection BAC Modification Kit (Gene Bridges, Heidelberg, Germany) according to manufacturer's instructions (32). The cDNA corresponding to the 3′-end of genomic RNA between nt 28046 and 28545 with 25 nts of adenine (pA) and partial HDV ribozyme (Rz) sequence was generated by chemical synthesis (Eurofins, Brussels, Belgium; this cDNA was used as a PCR template for synthesizing Fr8 (Fig. 1A). For synthesizing other fragments, RT-PCR was carried out using genomic RNA of the C3663 strain as described in "RNA extraction and RT-PCR." For Fr11 amplification, the reverse primer YT648 (5′-TTTGCCTTATAACTTCCGTAGGTGTAAACTCATCACATAATGAGCCATAAG ACA-3′) was designed to disrupt the *Eco*RI site of C3663 between nt 9829 and 9834

(Fig. 1B). The cDNA clone carrying the full-length C3663 sequence was designated as pBAC-FCoV-C3663. Sequence analysis of the full genome sequence of C3663 in pBAC-FCoV-C3663 was carried out by Eurofins. For construction of reporter rC3663, we replaced the ORF 3abc genes of pBAC-FCoV-C3663 with Nluc (Promega, Fitchburg, WI) using the recombination method described above (Fig. 2A) and designated the infectious cDNA clone as pBAC-FCoV-C3663-Nluc. The same recombination method was also applied for the construction of pBAC-FCoV-C3663-Nluc-PolDead, which possesses amino acid substitutions (SDD to SAA) at the active site of RdRp (nsp12; Fig. 4A).

RNA extraction and RT-PCR

Viral RNA from the viral stock of type I FCoV strain C3663 and rC3663 were extracted using the PureLink RNA Mini Kit (Thermo Fisher Scientific, Waltham, MA) according to manufacturer's instructions. RNA was reverse-transcribed using the SuperScript III First-Strand Synthesis System for RT-PCR (Invitrogen, Waltham, MA) with random hexamers according to manufacturer's instructions and PCR was carried out using PrimeSTAR GXL DNA Polymerase (TaKaRa, Shiga, Japan). C3663 cDNA was used as a PCR template for synthesizing the recombination template as described above. rC3663 cDNA was used for genetic marker confirmation.

Total RNA from rC3663 virus or mock-infected Fcwf-4 cells and A72 cells was isolated and reverse-transcribed as described above.

Plasmid construction

To obtain DIG-labeled riboprobes for detecting FCoV RNA via northern blot analysis,

469 we constructed the pSPT18-FCoV plasmid. The nucleotide sequence between nt 27803
470 and 28329 of the C3663 genome was cloned into the pSPT18 plasmid through ligation
471 using *Hind*III and *Eco*RI restriction sites (DNA Ligation Kit Mighty Mix; Takara).
472 Furthermore, we constructed the *Escherichia coli* expression plasmid
473 pGEX6P-1-3663N181-377/GST to produce GST-fused partial N protein. The nucleotide
474 sequence between nt 26745 and 27335, encoding amino acid residues 181–377 of
475 C3663, was inserted into pGEX6P-1 through ligation using *Bam*HI and *Xho*I restriction
476 sites (DNA Ligation Kit Mighty Mix).
477
478 **Rescue of rC3663 from susceptible Fcwf-4 cells**
479 Fcwf-4 cells were seeded onto 6-well plates (Violamo; Misumi, Schaumberg, IL) at 4.0
480 × 10^5 cells/well. After incubation at 37 °C overnight, the cells were transfected with 4
481 μg cDNA clones using XtremeGene 9 DNA Transfection Reagent (Roche, Basel,
482 Switzerland) according to manufacturer's instructions. After 3 days of culturing at
483 37 °C, CPE were observed and culture supernatants were harvested. The supernatants
484 were stored as P0 viruses. P0 viruses were passaged twice in fresh Fcwf-4 cells in
485 10-cm dishes (Violamo) and then P2 viruses were used for conducting experiments.
486
487 **rC3663 genetic marker confirmation**
488 To determine the genetic marker of rC3663, rC3663 cDNA was used as a template for
489 PCR using the primer pair YT649 (5′-GCATGCAACTGGAGGGTACT-3′) and YT650
490 (5′-AGAGGATAGCCAAAGCGGTC-3′) and PrimeSTAR GXL DNA Polymerase. PCR
491 products were purified using the HighPure PCR Purification Kit (Roche) and DNA
492 samples were treated with *Eco*RI at 37 °C overnight. Treated samples were then

electrophoresed and cleavage was verified. Purified DNA samples were also used for sequence analysis to confirm the genetic marker. Sequence analyses were carried out by Eurofins using the primer YT649.

Measurement of viral growth in Fcwf-4 cells and canine-derived A72, MDCK, and DH82 cells

Fcwf-4, A72, MDCK, and DH82 cells were seeded onto 6-well plates at 4.0×10^5, 2.0×10^5, 2.0×10^5, and 2.0×10^5 cells/well, respectively, and cultured at 37 °C overnight. Viruses were used to inoculate each cell line at MOI = 0.01. After adsorption at 37 °C for 1 h, the cells were washed twice with DMEM and then fresh DMEM containing 10% FBS was added. Infected cells were cultured at 37 °C for 24, 48, and 72 h and culture supernatants were collected and stored at -80 °C until further use in titration assays. Next, infected cells were collected and washed once using phosphate-buffered saline (PBS) and the cell pellets divided into two aliquots for real-time RT-PCR and western blot analysis.

Measurement of viral titers by the plaque assay

Fcwf-4 cells were seeded onto 6-well plates at 1.0×10^6 cells/well and cultured at 37 °C overnight. Samples were diluted with a 10-fold serial dilution from a 10X dilution using DMEM. Diluted viruses (400 µL) were added to the Fcwf-4 cells and incubated at 37 °C for 1 h for adsorption. After adsorption, supernatants were removed, and the cells were washed twice using DMEM. Next, 0.8% agarose (SeaPlaque GTG Agarose; Lonza, Basel, Switzerland) in DMEM containing 10% FBS was overlaid on to the infected cells and incubated at 37 °C until CPE were observed. Finally, infected cells were fixed

517 with phosphate-buffered formalin (Nacalai Tesque) and stained with crystal violet. The
518 number of plaques were then counted and viral titers calculated as plaque forming units
519 (PFU)/mL.
520
521 **Northern blot analysis**
522 RNA from C3663 or rC3663-infected Fcwf-4 cells were used for northern blot analysis
523 as described elsewhere (32). RNA samples were diluted to 2 µg in 5 µL by UltraPure
524 DW (Invitrogen) and then mixed with 5 µL 2X Loading Dye (New England Biolabs,
525 Ipswich, MA). After heating at 65 °C for 5 min, 10 µL RNA samples were
526 electrophoresed with 1.2% denaturing agarose gel and transferred onto a positively
527 charged nylon membrane (Roche). Northern blot analysis was performed using a DIG
528 Wash and Block Buffer Set and a DIG Luminescence Detection Kit (Roche).
529 DIG-labeled riboprobes for detecting viral RNAs were generated using pSPT18-FCoV
530 and a DIG RNA Labeling Kit (SP6/T7; Roche) as described previously (68, 69).
531
532 **Measurement of Nluc activity**
533 Fcwf-4 (1.0×10^5 cells/well), A72, MDCK, and DH82 (all 1.5×10^5 cells/well) cells
534 were seeded onto 24-well plates (Violamo) and cultured at 37 °C overnight. After
535 washing, rC3663-Nluc or rC3663 were inoculated at MOI = 0.01 or 0.1. After
536 adsorption, the cells were washed twice using DMEM and then fresh DMEM containing
537 10% FBS was added. The cells were then incubated at 37 °C for 24, 48, and 72 h, after
538 which culture supernatants were removed and cells lysed using passive buffer
539 (Promega). Luciferase activity was measured using the Nano-Glo Luciferase Assay
540 System (Promega) on a PowerScan HT (DS Pharma Biomedical, Osaka, Japan). The

experiments were carried out in triplicate.

Measurement of inhibitory effects against type I FCoV replication

Fcwf-4 cells were seeded onto 24-well plates at 1.0×10^5 cells/well and cultured at 37 °C overnight. After washing the cells, 100 µL rC3663-Nluc was used for inoculation at MOI = 0.01. After adsorption at 37°C for 1 h, the infected cells were washed twice with DMEM and then fresh DMEM supplemented with 10% FBS and different concentrations of cyclosporine A (Sigma-Aldrich, St. Louis, MO) or lopinavir (Sigma-Aldrich) was added. Using a 2-fold serial dilution with DMSO, cyclosporine A was diluted from 50 µM to 3.125 µM and lopinavir from 30 µM to 3.75 µM. DMSO was also used as control. After incubation at 37 °C for 24 h, culture supernatants were removed, and the cells lysed with passive buffer. Nluc activity was then measured as described above.

Compound screening using a protease inhibitor library

We used a chemical library of 68 compounds (L1100; Protease Inhibitor Library; TargetMol) (70) for compound screening. Fcwf-4 cells were seeded onto 96-well plates (Violamo) at 2.0×10^4 cells/well and cultured at 37 °C overnight. Mixtures containing rC3663-Nluc at MOI = 0.01 and 10 µM of each compound from the library in DMEM were prepared and added to the cultured Fcwf-4 cells. Cyclosporine A (10 µM) and DMSO were used as the positive and negative controls, respectively. After incubation for 24 h, the culture supernatants were removed and cells lysed in passive buffer. Nluc activity was measured as described above.

MTT assay

Fcwf-4 cells were seeded onto 96-well plates at 1.0×10^4 cells/well and cultured at 37 °C overnight. Each compound (10 μM in DMEM) from the protease inhibitor library was added to the cultured Fcwf-4 cells. After incubation for 24 h, MTT assays were carried out using the MTT Cell Count Kit (Nacalai Tesque) according to manufacturer's instructions. Absorbance at 570 nm was then measured with the PowerScan HT.

Real-time RT-PCR

Cell pellets of infected Fcwf-4, A72, MDCK, and DH82 cells were lysed and then total RNA was extracted using the PureLink RNA Mini Kit. RNA was then used for real-time RT-PCR with the Thunderbird Probe One-Step qPCR Mix (Toyobo, Osaka, Japan) and run on the StepOne Real-Time PCR System (Applied Biosystems, Waltham, MA). For quantification of FCoV RNA, we used the 3′-UTR targeting primers FcoV1128f (5′-GATTTGATTTGGCAATGCTAGATTT-3′; nt 28398–28422 of C3663) and FcoV1229r (5′-AACAATCACTAGATCCAGACGTTAGCT-3′; nt 28473–28499 of C3663) as well as a specific probe (5′-TCCATTGTTGGCTCGTCATAGCGGA-3′; nt 28446–28470 of C3663) labeled with FAM (71). For quantification of GAPDH mRNA, wk1288 (5′-GAAGGTGAAGGTCGGAGT-3′) and wk1289 (5′-GAAGATGGTGATGGGATTTC-3′) were used as primers and FAM-labeled wk1290 (5′-CAAGCTTCCCGTTCTCAGCC-3′) was used as a probe (32). Cycling conditions were 95 °C for 1 min, followed by 40 cycles of 95 °C for 15 s and 58 °C for 45 s.

Construction of monoclonal antibody against N protein of type I FCoV

GST-fused partial N protein, C3663N181-377/GST, was expressed in *Escherichia coli*

carrying pGEX6P-1-C3663N181-377/GST and purified using glutathione Sepharose 4B beads (GE healthcare, Chicago, IL). The purified protein was used as an antigen for immunization of Balb/c mice. The method of monoclonal antibody (mAb) establishment was described previously (72). Screening of hybridomas was performed by enzyme-linked immunosorbent assays (ELISA) using purified C3663N181-377/GST or GST proteins. ELISA was carried out as described previously (73). We yielded the clone designated as 4D10 which produced mAbs against type I FCoV N protein.

Western blot analysis

Infected Fcwf-4, A72, MDCK, and DH82 cells were lysed in lysis buffer (100 mM Tris-HCl pH 8.0, 150 mM NaCl, and 1% TritonX-100) and centrifuged at 16,000 × *g* for 10 min at 4 °C. Supernatants were then collected and mixed with 2X sample buffer (0.1 M Tris-HCl pH 6.8, 4% sodium dodecyl sulfate [SDS], 20% glycerol, 0.004% bromophenol blue, and 10% 2-mercaptoethanol). Next, the boiled samples were electrophoresed by SDS-polyacrylamide gel electrophoresis (PAGE) and transferred onto a polyvinylidene difluoride (PVDF) membrane (Merck Millipore, Billerica, MA). The membranes were blocked in 3% skim milk in PBS containing 0.05% Tween 20 (PBS-T; Nacalai Tesque). Primary antibodies were mouse anti-FCoV-N monoclonal antibody (4D10) and mouse anti-β-Actin antibody (Sigma-Aldrich), while goat anti-mouse IgG-horseradish peroxidase (HRP; Sigma-Aldrich) was used as a secondary antibody. ChemiLumi One Ultra (Nacalai Tesque) was used for visualization (32).

IFA

Fcwf-4 and A72 cells were seeded onto 35-mm glass bottom dishes (Matsunami Glass,

Osaka, Japan) at 2.0 × 10^5 or 1.0 × 10^5 cells/well, respectively. After incubation at 37 °C overnight, the cells were inoculated with rC3663 at MOI = 0.1. Following adsorption at 37 °C for 1 h, the supernatants were removed and fresh DMEM containing 10% FBS was added. The infected cells were cultured at 37 °C for 48 h and then fixed with 4% paraformaldehyde in PBS. After washing once with PBS, the cells were permeabilized for 15 min at room temperature with PBS containing 0.5% Triton X-100. The cells were then incubated with the mouse anti-FCoV-N monoclonal antibody 4D10 at 4 °C overnight, after which they were washed three times with PBS and incubated with CF488-conjugated anti-mouse IgG (1:500; Sigma-Aldrich) for 1 h at room temperature. Finally, the cells were washed three times with PBS and then Fluoroshield with DAPI (ImmunoBioScience, Mukilteo, WA) was used as a mounting medium and for nuclei counterstaining with DAPI. The cells were observed with the laser scanning confocal microscope FluoView FV1000 (Olympus, Tokyo, Japan)

Transfection of MDCK cells with pBAC-FCoV-Nluc

MDCK cells were seeded onto 24-well plates at 1.5 × 10^5 cells/well and cultured at 37 °C overnight. The cells were then transfected with 1 µg pBAC-FCoV-Nluc and 0.1 µg pcDNA3.1-fluc (32) using Lipofectamine 2000 (Thermo Fisher Scientific) according to manufacturer's instructions. pBAC-FCoV-Nluc-PolDead was used as control. Transfected cells were incubated at 37 °C for 6 h, after which the supernatants were removed and fresh DMEM containing 10% FBS was added. After incubating for an additional 18, 42, and 66 h, (i.e., 24, 48, and 72 h after transfection), culture supernatants were removed, and the cells lysed in passive buffer. Nluc and firefly luciferase activity were measured as described above and with the Luciferase Assay

637 System (Promega), respectively. Nluc activity was normalized to firefly luciferase
638 activity. For other virological tests (Fig. 4B–D), the experiment was scaled up from
639 24-well plates to 6-well plates.
640

641 **Acknowledgements**

642 We thank Dr Luis Enjuanes (CNB-CSIC, Madrid, Spain) for providing the
643 SARS-CoV-Rep BAC DNA. We also thank Ms. Kaede Yukawa for secretarial
644 assistance and Ms. Kanako Yoshizawa and Nozomi Shimada for their technical
645 assistance. This work was supported in part by grants-in-aid for the Research Program
646 on Emerging and Re-Emerging Infectious Diseases from the Japan Agency for Medical
647 Research and Development and Japanese Society for the Promotion of Science (JSPS)
648 KAKENHI grant JP16K08811, JP18fk0108058, and JP15J07066. YT was supported by
649 a JSPS Research Fellowship for young scientists. The authors have no potential
650 conflicts of interest in relation to this study.
651

652 **Reference**

653 1. Weiss SR, Navas-Martin S. 2005. Coronavirus pathogenesis and the emerging pathogen
654 severe acute respiratory syndrome coronavirus. Microbiol Mol Biol Rev 69:635-64.
655 2. Woo PC, Huang Y, Lau SK, Yuen KY. 2010. Coronavirus genomics and bioinformatics
656 analysis. Viruses 2:1804-20.
657 3. International Committee on Taxonomy of Viruses., King AMQ. 2012. Virus taxonomy :
658 classification and nomenclature of viruses : ninth report of the International
659 Committee on Taxonomy of Viruses. Academic Press, London ; Waltham, MA.
660 4. Biek R, Ruth TK, Murphy KM, Anderson CR, Jr., Johnson M, DeSimone R, Gray R,
661 Hornocker MG, Gillin CM, Poss M. 2006. Factors associated with pathogen
662 seroprevalence and infection in Rocky Mountain cougars. J Wildl Dis 42:606-15.
663 5. Hofmann-Lehmann R, Fehr D, Grob M, Elgizoli M, Packer C, Martenson JS, O'Brien
664 SJ, Lutz H. 1996. Prevalence of antibodies to feline parvovirus, calicivirus,

herpesvirus, coronavirus, and immunodeficiency virus and of feline leukemia virus antigen and the interrelationship of these viral infections in free-ranging lions in east Africa. Clin Diagn Lab Immunol 3:554-62.

6. Heeney JL, Evermann JF, McKeirnan AJ, Marker-Kraus L, Roelke ME, Bush M, Wildt DE, Meltzer DG, Colly L, Lukas J, et al. 1990. Prevalence and implications of feline coronavirus infections of captive and free-ranging cheetahs (Acinonyx jubatus). J Virol 64:1964-72.

7. Pedersen NC, Evermann JF, McKeirnan AJ, Ott RL. 1984. Pathogenicity studies of feline coronavirus isolates 79-1146 and 79-1683. Am J Vet Res 45:2580-5.

8. Holzworth J. 1963. Some important disorders of cats. Cornell Vet 53:157-60.

9. Terada Y, Shiozaki Y, Shimoda H, Mahmoud HY, Noguchi K, Nagao Y, Shimojima M, Iwata H, Mizuno T, Okuda M, Morimoto M, Hayashi T, Tanaka Y, Mochizuki M, Maeda K. 2012. Feline infectious peritonitis virus with a large deletion in the 5'-terminal region of the spike gene retains its virulence for cats. J Gen Virol 93:1930-4.

10. Fiscus SA, Teramoto YA. 1987. Antigenic comparison of feline coronavirus isolates: evidence for markedly different peplomer glycoproteins. J Virol 61:2607-13.

11. Hohdatsu T, Sasamoto T, Okada S, Koyama H. 1991. Antigenic analysis of feline coronaviruses with monoclonal antibodies (MAbs): preparation of MAbs which discriminate between FIPV strain 79-1146 and FECV strain 79-1683. Vet Microbiol 28:13-24.

12. Benetka V, Kubber-Heiss A, Kolodziejek J, Nowotny N, Hofmann-Parisot M, Mostl K. 2004. Prevalence of feline coronavirus types I and II in cats with histopathologically verified feline infectious peritonitis. Vet Microbiol 99:31-42.

13. Kummrow M, Meli ML, Haessig M, Goenczi E, Poland A, Pedersen NC, Hofmann-Lehmann R, Lutz H. 2005. Feline coronavirus serotypes 1 and 2: seroprevalence and association with disease in Switzerland. Clin Diagn Lab Immunol 12:1209-15.

14. Shiba N, Maeda K, Kato H, Mochizuki M, Iwata H. 2007. Differentiation of feline coronavirus type I and II infections by virus neutralization test. Vet Microbiol 124:348-52.

15. Hohdatsu T, Izumiya Y, Yokoyama Y, Kida K, Koyama H. 1998. Differences in virus receptor for type I and type II feline infectious peritonitis virus. Arch Virol 143:839-50.

16. Pedersen NC, Liu H, Dodd KA, Pesavento PA. 2009. Significance of coronavirus mutants in feces and diseased tissues of cats suffering from feline infectious peritonitis. Viruses 1:166-84.

17. Poland AM, Vennema H, Foley JE, Pedersen NC. 1996. Two related strains of feline infectious peritonitis virus isolated from immunocompromised cats infected with a feline enteric coronavirus. J Clin Microbiol 34:3180-4.
18. Vennema H, Poland A, Foley J, Pedersen NC. 1998. Feline infectious peritonitis viruses arise by mutation from endemic feline enteric coronaviruses. Virology 243:150-7.
19. Chang HW, Egberink HF, Halpin R, Spiro DJ, Rottier PJ. 2012. Spike protein fusion peptide and feline coronavirus virulence. Emerg Infect Dis 18:1089-95.
20. Licitra BN, Millet JK, Regan AD, Hamilton BS, Rinaldi VD, Duhamel GE, Whittaker GR. 2013. Mutation in spike protein cleavage site and pathogenesis of feline coronavirus. Emerg Infect Dis 19:1066-73.
21. Kiss I, Poland AM, Pedersen NC. 2004. Disease outcome and cytokine responses in cats immunized with an avirulent feline infectious peritonitis virus (FIPV)-UCD1 and challenge-exposed with virulent FIPV-UCD8. J Feline Med Surg 6:89-97.
22. Pedersen NC, Black JW. 1983. Attempted immunization of cats against feline infectious peritonitis, using avirulent live virus or sublethal amounts of virulent virus. Am J Vet Res 44:229-34.
23. Mochizuki M, Mitsutake Y, Miyanohara Y, Higashihara T, Shimizu T, Hohdatsu T. 1997. Antigenic and plaque variations of serotype II feline infectious peritonitis coronaviruses. J Vet Med Sci 59:253-8.
24. Eckert N, Wrensch F, Gartner S, Palanisamy N, Goedecke U, Jager N, Pohlmann S, Winkler M. 2014. Influenza A virus encoding secreted Gaussia luciferase as useful tool to analyze viral replication and its inhibition by antiviral compounds and cellular proteins. PLoS One 9:e97695.
25. Tran V, Moser LA, Poole DS, Mehle A. 2013. Highly sensitive real-time in vivo imaging of an influenza reporter virus reveals dynamics of replication and spread. J Virol 87:13321-9.
26. Tekes G, Hofmann-Lehmann R, Stallkamp I, Thiel V, Thiel HJ. 2008. Genome organization and reverse genetic analysis of a type I feline coronavirus. J Virol 82:1851-9.
27. de Wilde AH, Zevenhoven-Dobbe JC, van der Meer Y, Thiel V, Narayanan K, Makino S, Snijder EJ, van Hemert MJ. 2011. Cyclosporin A inhibits the replication of diverse coronaviruses. J Gen Virol 92:2542-8.
28. Pfefferle S, Schopf J, Kogl M, Friedel CC, Muller MA, Carbajo-Lozoya J, Stellberger T, von Dall'Armi E, Herzog P, Kallies S, Niemeyer D, Ditt V, Kuri T, Zust R, Pumpor K, Hilgenfeld R, Schwarz F, Zimmer R, Steffen I, Weber F, Thiel V, Herrler G, Thiel

HJ, Schwegmann-Wessels C, Pohlmann S, Haas J, Drosten C, von Brunn A. 2011. The SARS-coronavirus-host interactome: identification of cyclophilins as target for pan-coronavirus inhibitors. PLoS Pathog 7:e1002331.

29. de Wilde AH, Jochmans D, Posthuma CC, Zevenhoven-Dobbe JC, van Nieuwkoop S, Bestebroer TM, van den Hoogen BG, Neyts J, Snijder EJ. 2014. Screening of an FDA-approved compound library identifies four small-molecule inhibitors of Middle East respiratory syndrome coronavirus replication in cell culture. Antimicrob Agents Chemother 58:4875-84.

30. Boyle JF, Pedersen NC, Evermann JF, McKeirnan AJ, Ott RL, Black JW. 1984. Plaque assay, polypeptide composition and immunochemistry of feline infectious peritonitis virus and feline enteric coronavirus isolates. Adv Exp Med Biol 173:133-47.

31. McKeirnan AJ, Evermann JF, Davis EV, Ott RL. 1987. Comparative properties of feline coronaviruses in vitro. Can J Vet Res 51:212-6.

32. Terada Y, Kawachi K, Matsuura Y, Kamitani W. 2017. MERS coronavirus nsp1 participates in an efficient propagation through a specific interaction with viral RNA. Virology 511:95-105.

33. Millet JK, Whittaker GR. 2015. Host cell proteases: Critical determinants of coronavirus tropism and pathogenesis. Virus Res 202:120-34.

34. Yamamoto M, Matsuyama S, Li X, Takeda M, Kawaguchi Y, Inoue JI, Matsuda Z. 2016. Identification of Nafamostat as a Potent Inhibitor of Middle East Respiratory Syndrome Coronavirus S Protein-Mediated Membrane Fusion Using the Split-Protein-Based Cell-Cell Fusion Assay. Antimicrob Agents Chemother 60:6532-6539.

35. Walmsley S, Bernstein B, King M, Arribas J, Beall G, Ruane P, Johnson M, Johnson D, Lalonde R, Japour A, Brun S, Sun E, Team MS. 2002. Lopinavir-ritonavir versus nelfinavir for the initial treatment of HIV infection. N Engl J Med 346:2039-46.

36. Hsieh LE, Lin CN, Su BL, Jan TR, Chen CM, Wang CH, Lin DS, Lin CT, Chueh LL. 2010. Synergistic antiviral effect of Galanthus nivalis agglutinin and nelfinavir against feline coronavirus. Antiviral Res 88:25-30.

37. Kim Y, Mandadapu SR, Groutas WC, Chang KO. 2013. Potent inhibition of feline coronaviruses with peptidyl compounds targeting coronavirus 3C-like protease. Antiviral Res 97:161-8.

38. Takano T, Katoh Y, Doki T, Hohdatsu T. 2013. Effect of chloroquine on feline infectious peritonitis virus infection in vitro and in vivo. Antiviral Res 99:100-7.

773 39. Fischer Y, Ritz S, Weber K, Sauter-Louis C, Hartmann K. 2011. Randomized, placebo
774 controlled study of the effect of propentofylline on survival time and quality
775 of life of cats with feline infectious peritonitis. J Vet Intern Med 25:1270-6.
776 40. Pedersen NC. 2014. An update on feline infectious peritonitis: diagnostics and
777 therapeutics. Vet J 201:133-41.
778 41. Olsen CW, Corapi WV, Ngichabe CK, Baines JD, Scott FW. 1992. Monoclonal antibodies
779 to the spike protein of feline infectious peritonitis virus mediate
780 antibody-dependent enhancement of infection of feline macrophages. J Virol
781 66:956-65.
782 42. Takano T, Kawakami C, Yamada S, Satoh R, Hohdatsu T. 2008. Antibody-dependent
783 enhancement occurs upon re-infection with the identical serotype virus in feline
784 infectious peritonitis virus infection. J Vet Med Sci 70:1315-21.
785 43. Jacobse-Geels HE, Daha MR, Horzinek MC. 1980. Isolation and characterization of
786 feline C3 and evidence for the immune complex pathogenesis of feline infectious
787 peritonitis. J Immunol 125:1606-10.
788 44. Jacobse-Geels HE, Daha MR, Horzinek MC. 1982. Antibody, immune complexes, and
789 complement activity fluctuations in kittens with experimentally induced feline
790 infectious peritonitis. Am J Vet Res 43:666-70.
791 45. Herrewegh AA, Smeenk I, Horzinek MC, Rottier PJ, de Groot RJ. 1998. Feline
792 coronavirus type II strains 79-1683 and 79-1146 originate from a double
793 recombination between feline coronavirus type I and canine coronavirus. J Virol
794 72:4508-14.
795 46. Terada Y, Matsui N, Noguchi K, Kuwata R, Shimoda H, Soma T, Mochizuki M, Maeda
796 K. 2014. Emergence of pathogenic coronaviruses in cats by homologous recombination
797 between feline and canine coronaviruses. PLoS One 9:e106534.
798 47. Pratelli A, Martella V, Decaro N, Tinelli A, Camero M, Cirone F, Elia G, Cavalli
799 A, Corrente M, Greco G, Buonavoglia D, Gentile M, Tempesta M, Buonavoglia C. 2003.
800 Genetic diversity of a canine coronavirus detected in pups with diarrhoea in Italy.
801 J Virol Methods 110:9-17.
802 48. Decaro N, Mari V, Campolo M, Lorusso A, Camero M, Elia G, Martella V, Cordioli
803 P, Enjuanes L, Buonavoglia C. 2009. Recombinant canine coronaviruses related to
804 transmissible gastroenteritis virus of Swine are circulating in dogs. J Virol
805 83:1532-7.
806 49. Tresnan DB, Levis R, Holmes KV. 1996. Feline aminopeptidase N serves as a receptor
807 for feline, canine, porcine, and human coronaviruses in serogroup I. J Virol
808 70:8669-74.

809 50. Pratelli A, Decaro N, Tinelli A, Martella V, Elia G, Tempesta M, Cirone F,
810 Buonavoglia C. 2004. Two genotypes of canine coronavirus simultaneously detected
811 in the fecal samples of dogs with diarrhea. J Clin Microbiol 42:1797-9.
812 51. Matsuyama S, Nagata N, Shirato K, Kawase M, Takeda M, Taguchi F. 2010. Efficient
813 activation of the severe acute respiratory syndrome coronavirus spike protein by
814 the transmembrane protease TMPRSS2. J Virol 84:12658-64.
815 52. Verheije MH, Raaben M, Mari M, Te Lintelo EG, Reggiori F, van Kuppeveld FJ, Rottier
816 PJ, de Haan CA. 2008. Mouse hepatitis coronavirus RNA replication depends on
817 GBF1-mediated ARF1 activation. PLoS Pathog 4:e1000088.
818 53. Wu CH, Chen PJ, Yeh SH. 2014. Nucleocapsid phosphorylation and RNA helicase DDX1
819 recruitment enables coronavirus transition from discontinuous to continuous
820 transcription. Cell Host Microbe 16:462-72.
821 54. Han HJ, Wen HL, Zhou CM, Chen FF, Luo LM, Liu JW, Yu XJ. 2015. Bats as reservoirs
822 of severe emerging infectious diseases. Virus Res 205:1-6.
823 55. Li W, Shi Z, Yu M, Ren W, Smith C, Epstein JH, Wang H, Crameri G, Hu Z, Zhang H,
824 Zhang J, McEachern J, Field H, Daszak P, Eaton BT, Zhang S, Wang LF. 2005. Bats
825 are natural reservoirs of SARS-like coronaviruses. Science 310:676-9.
826 56. Annan A, Baldwin HJ, Corman VM, Klose SM, Owusu M, Nkrumah EE, Badu EK, Anti P,
827 Agbenyega O, Meyer B, Oppong S, Sarkodie YA, Kalko EK, Lina PH, Godlevska EV,
828 Reusken C, Seebens A, Gloza-Rausch F, Vallo P, Tschapka M, Drosten C, Drexler JF.
829 2013. Human betacoronavirus 2c EMC/2012-related viruses in bats, Ghana and Europe.
830 Emerg Infect Dis 19:456-9.
831 57. Lau SKP, Wong EYM, Tsang CC, Ahmed SS, Au-Yeung RKH, Yuen KY, Wernery U, Woo PCY.
832 2018. Discovery and Sequence Analysis of Four Deltacoronaviruses from Birds in
833 the Middle East Reveal Interspecies Jumping with Recombination as a Potential
834 Mechanism for Avian-to-Avian and Avian-to-Mammalian Transmission. J Virol 92.
835 58. Vijgen L, Keyaerts E, Moes E, Thoelen I, Wollants E, Lemey P, Vandamme AM, Van
836 Ranst M. 2005. Complete genomic sequence of human coronavirus OC43: molecular clock
837 analysis suggests a relatively recent zoonotic coronavirus transmission event.
838 J Virol 79:1595-604.
839 59. van Hemert MJ, van den Worm SH, Knoops K, Mommaas AM, Gorbalenya AE, Snijder EJ.
840 2008. SARS-coronavirus replication/transcription complexes are
841 membrane-protected and need a host factor for activity in vitro. PLoS Pathog
842 4:e1000054.
843 60. Sola I, Mateos-Gomez PA, Almazan F, Zuniga S, Enjuanes L. 2011. RNA-RNA and
844 RNA-protein interactions in coronavirus replication and transcription. RNA Biol

8:237-48.

61. Ehmann R, Kristen-Burmann C, Bank-Wolf B, Konig M, Herden C, Hain T, Thiel HJ, Ziebuhr J, Tekes G. 2018. Reverse Genetics for Type I Feline Coronavirus Field Isolate To Study the Molecular Pathogenesis of Feline Infectious Peritonitis. MBio 9.

62. Jacobse-Geels HE, Horzinek MC. 1983. Expression of feline infectious peritonitis coronavirus antigens on the surface of feline macrophage-like cells. J Gen Virol 64 (Pt 9):1859-66.

63. Binn LN, Marchwicki RH, Stephenson EH. 1980. Establishment of a canine cell line: derivation, characterization, and viral spectrum. Am J Vet Res 41:855-60.

64. Nakano H, Kameo Y, Andoh K, Ohno Y, Mochizuki M, Maeda K. 2009. Establishment of canine and feline cells expressing canine signaling lymphocyte activation molecule for canine distemper virus study. Vet Microbiol 133:179-83.

65. Gaush CR, Hard WL, Smith TF. 1966. Characterization of an established line of canine kidney cells (MDCK). Proc Soc Exp Biol Med 122:931-5.

66. Wellman ML, Krakowka S, Jacobs RM, Kociba GJ. 1988. A macrophage-monocyte cell line from a dog with malignant histiocytosis. In Vitro Cell Dev Biol 24:223-9.

67. Almazán F, Dediego ML, Galán C, Escors D, Álvarez E, Ortego J, Sola I, Zuñiga S, Alonso S, Moreno JL, Nogales A, Capiscol C, Enjuanes L. 2006. Construction of a severe acute respiratory syndrome coronavirus infectious cDNA clone and a replicon to study coronavirus RNA synthesis. J Virol 80:10900-6.

68. Kamitani W, Narayanan K, Huang C, Lokugamage K, Ikegami T, Ito N, Kubo H, Makino S. 2006. Severe acute respiratory syndrome coronavirus nsp1 protein suppresses host gene expression by promoting host mRNA degradation. Proc Natl Acad Sci U S A 103:12885-90.

69. Tanaka T, Kamitani W, DeDiego ML, Enjuanes L, Matsuura Y. 2012. Severe acute respiratory syndrome coronavirus nsp1 facilitates efficient propagation in cells through a specific translational shutoff of host mRNA. J Virol 86:11128-37.

70. Tamura T, Fukuhara T, Uchida T, Ono C, Mori H, Sato A, Fauzyah Y, Okamoto T, Kurosu T, Setoh YX, Imamura M, Tautz N, Sakoda Y, Khromykh AA, Chayama K, Matsuura Y. 2018. Characterization of Recombinant Flaviviridae Viruses Possessing a Small Reporter Tag. J Virol 92.

71. Gut M, Leutenegger CM, Huder JB, Pedersen NC, Lutz H. 1999. One-tube fluorogenic reverse transcription-polymerase chain reaction for the quantitation of feline coronaviruses. J Virol Methods 77:37-46.

72. Shimoda H, Mahmoud HY, Noguchi K, Terada Y, Takasaki T, Shimojima M, Maeda K. 2013.

Production and characterization of monoclonal antibodies to Japanese encephalitis virus. J Vet Med Sci 75:1077-80.

73. Shimoda H, Inthong N, Noguchi K, Terada Y, Nagao Y, Shimojima M, Takasaki T, Rerkamnuaychoke W, Maeda K. 2013. Development and application of an indirect enzyme-linked immunosorbent assay for serological survey of Japanese encephalitis virus infection in dogs. J Virol Methods 187:85-9.

Figure Legends

Fig. 1 Constructing type I FCoV strain C3663 cDNA clones. (A) Schematic diagram illustrating the strategy for constructing infectious cDNA clones bearing the full-length genome of type I FCoV strain C3663. The full-length C3663 sequence was divided into

11 fragments (Fr1–Fr11) and each fragment was sequentially assembled into the plasmid backbone. * indicates the site of the genetic marker. (B) Nt sequence of the C3663 genome between nt 9826 and nt 9837. The *Eco*RI restriction site is underlined. rFCoV was mutated from GAATTC to GAGTTT for disrupting the *Eco*RI site (ΔEcoRI) to use as a genetic marker. Mutated nts are shown in gray boxes with white letters. (C) Confirmation of the genetic marker in the rC3663 genome by *Eco*RI treatment. RT-PCR products of parental virus C3663 and rC3663 that amplified a region including the genetic marker were treated with *Eco*RI. Treated samples were electrophoresed to confirm disruption of the *Eco*RI site in the rC3663 genome. (D) Sequence analysis of C3663 and rC3663 at the genetic marker site. The *Eco*RI restriction site and ΔEcoRI genetic marker are underlined. (E) Growth kinetics of parental virus C3663 and rC3663 in Fcwf-4 cells. Each virus was inoculated onto Fcwf-4 cells at MOI = 0.01 and incubated for 24, 48, and 72 h. Viral titers of culture supernatants were measured by plaque assays using Fcwf-4 cells. LOD, limit of detection. The data represent the mean ± SD of three independent experiments. (F) Northern blot analysis for detecting viral RNA in C3663 or rC3663-infected Fcwf-4 cells. Total RNA from Fcwf-4 cells infected with parental C3663 or rC3663 were extracted and electrophoresed. The transferred viral RNAs were hybridized with

DIG-labeled RNA targeting ORF 7b and 3′-UTR. gRNA, genomic RNA; sgRNA, subgenomic RNA.

Fig. 2 Construction and characteristics of the reporter virus carrying the Nluc gene. (A) Nluc gene replacement occurred at ORF 3abc to construct pBAC-FCoV-C3663-Nluc. Nluc gene replaced the start codon of ORF 3a to 71 nt upstream of the ORF 3c stop codon to retain the TRS of the E gene. Light gray, gray, and white boxes indicate non-structural proteins, structural proteins, and accessory proteins, respectively. TRS, transcription regulatory sequence. (B) Luciferase activity of rC3663-Nluc-infected cells. rC3663-Nluc and rC3663 were inoculated onto Fcwf-4 cells at MOI = 0.01 and incubated for 24, 48, and 72 h. Infected cells were lysed and luciferase activity was measured. Experiments were carried out in triplicate. (C) Growth kinetics of rC3663-Nluc. rC3663-Nluc and rC3663 were inoculated in Fcwf-4 cells at MOI = 0.01 and incubated for 24, 48, and 72 h. Viral titers of culture supernatants were measured by plaque assays using Fcwf-4 cells. LOD, limit of detection. (D, E) Evaluation of the inhibitory effects of (D) cyclosporine A and (E) lopinavir against rC3663-Nluc. Fcwf-4 cells were inoculated with rC3663-Nluc at MOI = 0.01. After adsorption, the viruses were removed and replaced by culture medium with or without

different concentrations of (D) cyclosporine A or (E) lopinavir. After incubation for 24 h, luciferase activities (black circle) or viral RNA (white triangle) were measured. The experiments were carried out in triplicate. (F) Compound screening using rC3663-Nluc and evaluation of the cytotoxicity of protease inhibitors by MTT assays. Sixty-eight protease inhibitors were used in this screening. Virus at MOI = 0.01 was added onto cultured Fcwf-4 cells with 10 μM of each protease inhibitor or DMSO and further cultured for 24 h. Cyclosporine A (CsA; 10 μM) was used as a positive control. Infected cell was lysed and Nluc activities were measured (bar graphs). For MTT assays, seeded Fcwf-4 cells were cultured with DMEM containing 10% FBS and 10 μM of each compound for 24 h. Then, cultured cells underwent MTT assays and the absorbance was measured at 570 nm (line graph). The data represent the mean ± SD of three independent experiments.

Fig. 3 Investigation of the infectivity of type I FCoV in canine-derived cell lines. (A, B) Infectivity of rC3663-Nluc in canine-derived cell lines. (A) Fcwf-4 cells and canine-derived A72 as well as (B) MDCK and DH82 cells were inoculated with mock or rC3663-Nluc (Nluc) at MOI = 0.1 and incubated for 24, 48, and 72 h. After incubation, infected cells were lysed and Nluc activities were measured. The

961 experiments were carried out in triplicate. (C) Cytopathic effects in Fcwf-4 and A72
962 cells infected with rC3663-Nluc. Fcwf-4 and A72 cells were inoculated with mock or
963 rC3663-Nluc (Nluc) at MOI = 0.1 and incubated for 24, 48, and 72 h. (D) Real-time
964 RT-PCR for the evaluation of viral RNA replication. Fcwf-4, A72, MDCK, and DH82
965 cells were inoculated with rC3663 at MOI = 0.01. Total RNA was extracted from the
966 infected cells and real-time RT-PCR targeting the 3′-UTR was carried out. (E) Growth
967 kinetics of rC3663 in Fcwf-4, A72, MDCK, and DH82 cells. rC3663 was used to
968 inoculate the cells at MOI = 0.01 and incubated for 24, 48, and 72 h. The culture
969 supernatants were collected at each time point and viral titers were measured by plaque
970 assays using Fcwf-4 cells. LOD, limit of detection. (F) Detection of rC3663 N protein in
971 Fcwf-4 and A72 cells by IFA. rC3663 was used to inoculate Fcwf-4 and A72 cells at
972 MOI = 0.1. Infected cells were incubated for 48 h. Then, infected cells were fixed with
973 4% paraformaldehyde. Fixed cells were treated with mouse anti-FCoV N monoclonal
974 antibody (primary antibody) and CF488-conjugated anti-mouse IgG (secondary
975 antibody). (G) Western blot analysis for the detection of rC3663 N protein. Cell lysates
976 of Fcwf-4, A72, MDCK, and DH82 cells infected with rC3663 were subjected to
977 western blot analysis using anti-FCoV N monoclonal antibody (a-N) and anti-actin
978 antibody (a-actin). Short and Long indicate short and long exposure, respectively. The

979 data represent the mean ± SD of three independent experiments.

980

981 **Fig. 4 Investigation of the resistance against type I FCoV infection.** (A) Strategy for
982 construction of polymerase dead mutant cDNA clones;
983 pBAC-FCoV-C3663-Nluc-PolDead (PolDead). * indicates the active site of viral RNA
984 dependent RNA polymerase (RdRp: nsp12). Nucleotide sequence of C3663 genome
985 between nt 14592 and nt 14612; mutated nts are shown in gray boxes with white letters.
986 pBAC-FCoV-C3663-Nluc (rC3663-Nluc) or pBAC-FCoV-C3663-Nluc-PolDead
987 (PolDead) were transfected into seeded MDCK cells. Transfected cells were incubated
988 for 24, 48, and 72 h. (B) At each time point, the transfected cells were lysed and Nluc
989 activities measured. As an internal control, firefly luciferase reporter plasmid,
990 pcDNA3.1-fluc, was co-transfected with BAC plasmids. Nluc activity was normalized
991 to the activity of firefly luciferase. (C) The culture supernatants at each time point were
992 collected and viral titers were measured by plaque assays using Fcwf-4 cells. LOD,
993 limit of detection. The experiments were carried out in triplicate. (D) Total RNA was
994 extracted from transfected MDCK cells and the levels of viral RNA were determined by
995 real-time RT-PCR. (E) Cell lysates of transfected MDCK cells were subjected to
996 western blot analysis using anti-FCoV N monoclonal antibody (a-N) and anti-actin

997 antibody (a-Actin). The data represent the mean ± SD of three independent experiments.

998

999 **Fig. 5 Aberrant expression of viral RNA of type I FCoV in A72 cells.**

1000 (A) Northern blot analysis for the detection of viral RNAs in rC3663, parental C3663,
1001 or Yayoi-infected A72 and Fcwf-4 cells. Total RNA from infected cells was extracted
1002 and electrophoresed. Viral RNAs were then hybridized with DIG-labeled RNA targeting
1003 ORF 7b and 3′-UTR. gRNA, genomic RNA; sgRNA, subgenomic RNA. (B) Diagram
1004 illustrating the DIG-labeled RNA probes used in northern blot analysis. (C) Northern
1005 blot analysis using S, 3abc, M, and N probes for detecting viral RNA in rC3663-infected
1006 Fcwf4-cells. Arrow indicates unknown RNA signal. (D) Northern blot analysis for
1007 detecting viral RNA in rC3663-infected Fcwf-4 and A72 cells. First lane, 0.05 μg of
1008 total RNA extracted from infected Fcwf-4 cells; second lane, 2 μg of total RNA
1009 extracted from infected A72 cells.

1010

1011

Table 1 Mutations in pBAC-FCoV

#	nt position	gene	nt mutation	aa mutation
1	2889	1a	C → T	Synonymous
2	6381	1a	C → T	Synonymous
3	6645	1a	G → T	K → N
4	9831	1a	A → G	Synonymous
5	9834	1a	C → T	Synonymous
6	12841	1b	T → C	V → A
7	17870	1b	C → T	Synonymous
8	18065	1b	C → T	Synonymous
9	18169	1b	C → T	A → V
10	21563	S	G → A	D → N
11	21976	S	T → C	Synonymous
12	22319	S	A → G	M → V
13	22619	S	G → A	E → K
14	23049	S	G → A	G → E
15	23473	S	C → T	Synonymous
16	23757	S	G → A	G → E
17	24500	3c	G → A	R → H
18	24608	3c	C → T	S → F
19	25220	E	C → T	Synonymous
20	25353	E	C → T	T → M
21	25928	M	A → G	Synonymous
22	26279	N	C → T	Synonymous
23	26442	N	G → A	E → K
24	27315	N	G → A	V → I
25	27634	7a	T → G	S → A

Table 2 Compound library of protease inhibitors

No.	ID	Name	CAS	Formula
1	T2316	MK3102	1226781-44-7	$C_{17}H_{20}F_2N_4O_3S$
2	T1772	Apoptosis Activator 2	79183-19-0	$C_{15}H_9Cl_2NO_2$
3	T1581	Picolamine	3731-52-0	$C_6H_8N_2$
4	T2893	Muscone	541-91-3	$C_{16}H_{30}O$
5	T0429	Glucosamine	3416-24-8	$C_6H_{13}NO_5$
6	T0372	Gabexate mesylate	56974-61-9	$C_{17}H_{27}N_3O_7$
7	T0087L	Sulfacetamide sodium	127-56-0	$C_8H_9N_2NaO_3S$
8	T0127	Glimepiride	93479-97-1	$C_{24}H_{34}N_4O_5S$
9	T0178	Saxagliptin hydrate	945667-22-1	$C_{18}H_{25}N_3O_2.H2O$
10	T0191	Linagliptin	668270-12-0	$C_{25}H_{28}N_8O_2$
11	T0242	Sitagliptin	486460-32-6	$C_{16}H_{15}F_6N_5O$
12	T0984	Fluorouracil (5-Fluoracil, 5-FU)	51-21-8	$C_4H_3FN_2O_2$
13	T1140	Doxycycline HCl	10592-13-9	$C_{22}H_{24}N_2O_8.HCl$
14	T1149	Fenofibrate	49562-28-9	$C_{20}H_{21}ClO_4$
15	T1366	3-Pyridylacetic acid hydrochloride	6419-36-9	$C_7H_8ClNO_2$
16	T2731	Usnic Acid	125-46-2	$C_{18}H_{16}O_7$
17	T2728	Limonin	1180-71-8	$C_{26}H_{30}O_8$
18	T2830	Betulinic acid	472-15-1	$C_{29}H_{46}O_3$
19	T2754	Oxymatrine	16837-52-8	$C_{15}H_{24}N_2O_2$
20	T2888	Pterostilbene	537-42-8	$C_{16}H_{16}O_3$
21	T0789	PMSF	329-98-6	$C_7H_7FO_2S$
22	T0951	Hydroxychloroquine sulfate	747-36-4	$C_{18}H_{26}ClN_3O.H_2SO_4$
23	T1402	Fenofibric acid	42017-89-0	$C_{17}H_{15}ClO_4$
24	T1462	Captopril	62571-86-2	$C_9H_{15}NO_3S$
25	T1525	Ritonavir	155213-67-5	$C_{37}H_{48}N_6O_5S_2$
26	T1564	Cisplatin	15663-27-1	$H_6C_{l2}N_2Pt$
27	T2843	Aloe-emodin	481-72-1	$C_{15}H_{10}O_5$
28	T2401	Alogliptin Benzoate	850649-62-6	$C_{25}H_{27}N_5O_4$
29	T2399	Bortezomib (PS-341)	179324-69-7	$C_{19}H_{25}BN_4O_4$
30	T1592	Acetohydroxamic acid	546-88-3	$C_2H_5NO_2$
31	T1623	Lopinavir	192725-17-0	$C_{37}H_{48}N_4O_5$
32	T2296	SYR472	1029877-94-8	$C_{22}H_{26}FN_5O_6$
33	T2262	GHF-5074	749269-83-8	$C_{16}H_{11}Cl_2FO_2$

34	T2016	MLN9708	1201902-80-8	$C_{20}H_{23}BCl_2N_2O_9$
35	T2122	MLN2238(Ixazomib)	1072833-77-2	$C_{14}H_{19}BCl_2N_2O_4$
36	T2239	Raltegravir potassium	871038-72-1	$C_{20}H_{20}FN_6O_5.K$
37	T2117	PSI6206	863329-66-2	$C_{10}H_{13}FN_2O_5$
38	T2392	Nafamostat mesylate	82956-11-4	$C_{19}H_{17}N_5O_2.2CH_4O_3S$
39	T1786	Daclatasvir, BMS790052	1009119-65-6	$C_{40}H_{52}Cl_2N_8O_6$
40	T2324 (T3335)	Darunavir Ethanolate	635728-49-3	$C_{27}H_{37}N_3O_7S.C_2H_5OH$
41	T2743	Ilomastat (GM6001, Galardin)	142880-36-2	$C_{20}H_{28}N_4O_4$
42	T2332	Elvitegravir (GS-9137, JTK-303)	697761-98-1	$C_{23}H_{23}ClFNO_5$
43	T2329	Dolutegravir (GSK1349572)	1051375-19-9	$C_{20}H_{18}F_2N_3NaO_5$
44	T2834	Nobiletin	478-01-3	$C_{21}H_{22}O_8$
45	T3028	Celastrol	34157-83-0	$C_{29}H_{38}O_4$
46	T2792	Glucosamine sulfate	29031-19-4	$C_6H_{13}NO_5.H_2SO_4$
47	T0100	Atazanavir sulfate	229975-97-7	$C_{38}H_{52}N_6O_7.H_2SO_4$
48	T1853	NMS 873	1418013-75-8	$C_{27}H_{28}N_4O_3S_2$
49	T1822	Clemizole	442-52-4	$C_{19}H_{20}ClN_3$
50	T1795	Carfilzomib (PR-171)	868540-17-4	$C_{40}H_{57}N_5O_7$
51	T0100L	Atazanavir	198904-31-3	$C_{38}H_{52}N_6O_7$
52	T1502	Vildagliptin (LAF-237)	274901-16-5	$C_{17}H_{25}N_3O_2$
54	T2009	SB-3CT	292605-14-2	$C_{15}H_{14}O_3S_2$
55	T1757	ML323	1572414-83-5	$C_{23}H_{24}N_6$
56	T2424	P22077	1247819-59-5	$C_{12}H_7F_2NO_3S_2$
57	T2493	PD 151746	179461-52-0	$C_{11}H_8FNO_2S$
58	T2503	PAC1	315183-21-2	$C_{23}H_{28}N_4O_2$
59	T2393	Efavirenz	154598-52-4	$C_{14}H_9ClF_3NO_2$
60	T1883	Des(benzylpyridyl) Atazanavi	1192224-24-0	$C_{26}H_{43}N_5O_7$
61	T1862	PR-619	2645-32-1	$C_7H_5N_5S_2$
62	T2625	MK0752	471905-41-6	$C_{21}H_{21}ClF_2O_4S$
63	T2639	LY2811376	1194044-20-6	$C_{15}H_{14}F_2N_4S$
64	T3075	FLI-06	313967-18-9	$C_{25}H_{30}N_2O_5$
65	T1969	DBEQ	177355-84-9	$C_{22}H_{20}N_4$
66	T1932	B-AP15	1009817-63-3	$C_{22}H_{17}N_3O_6$
67	T1924	LDN-57444	668467-91-2	$C_{17}H_{11}Cl_3N_2O_3$

68	T1891	NSC 405020	7497-07-6	$C_{12}H_{15}Cl_2NO$
69	T2154	MG-132	133407-82-6	$C_{26}H_{41}N_3O_5$

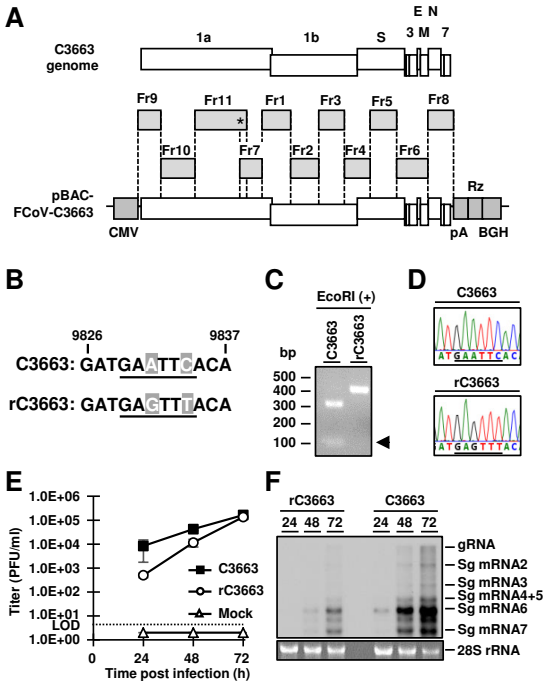

Figure 1. Y Terada, et al,.

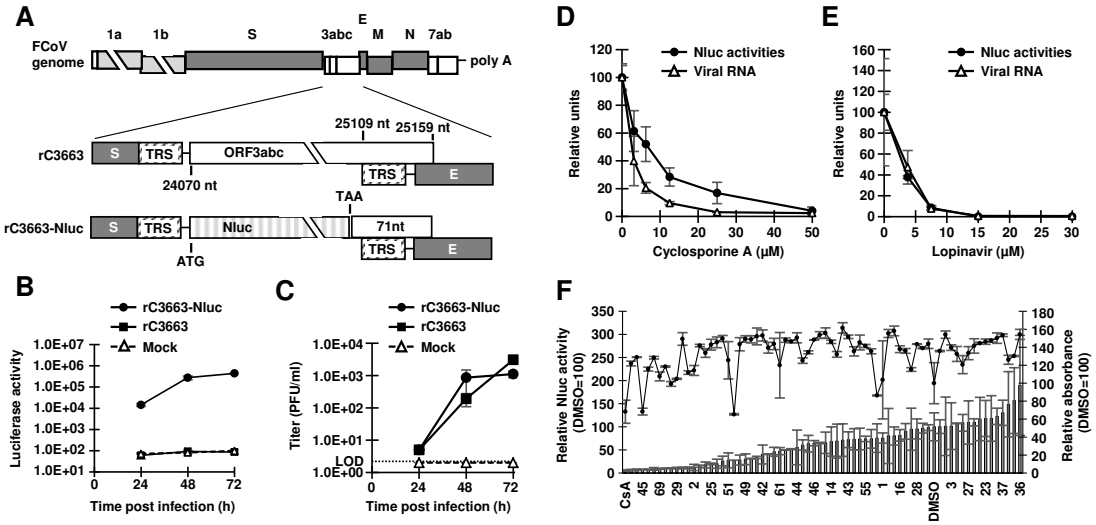

Figure 2. Y Terada, et al,.

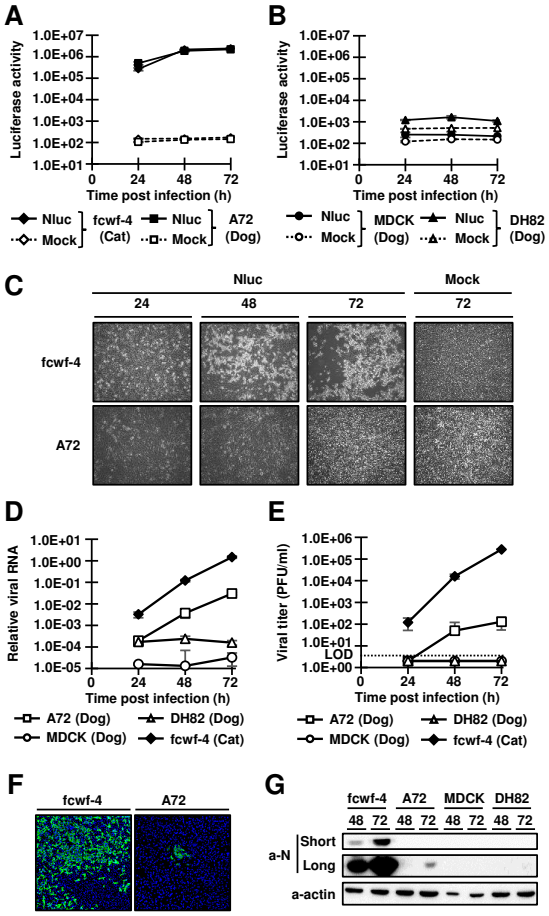

Figure 3. Y Terada, et al,.

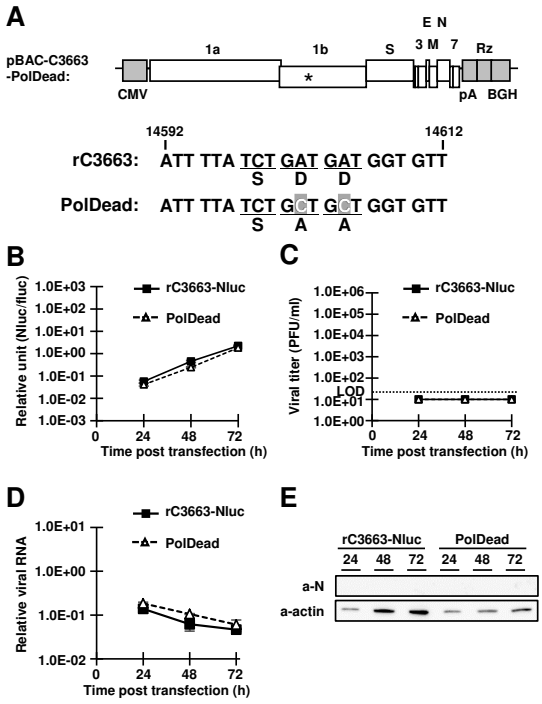

Figure 4. Y Terada, et al,.

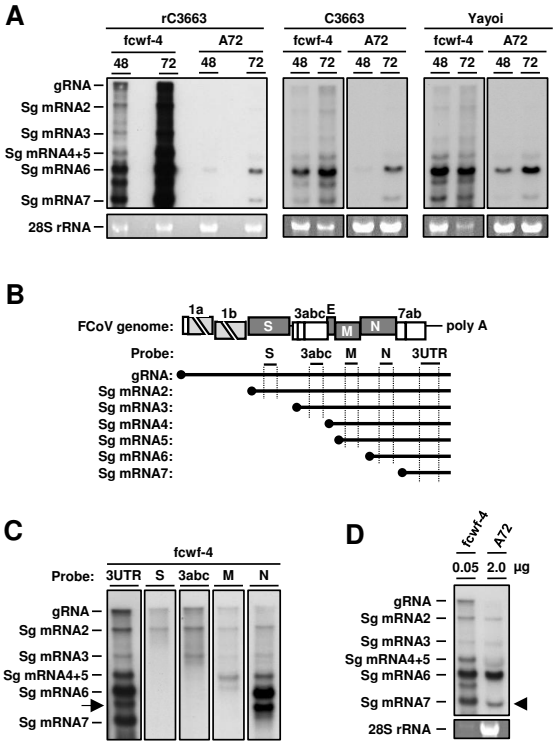

Figure 5. Y Terada, et al,.